Sensitivity analysis for mercury over Europe

Yelva Roustan, Marc Bocquet

Sensitivity analysis for mercury over Europe

Yelva Roustan and Marc Bocquet

CEREA, Research and Teaching Center in Atmospheric Environment,
Joint laboratory, École Nationale des Ponts et Chaussées / EDF R&D,
avenue Blaise Pascal, 77455 Champs sur Marne, France

Abstract. Adjoint techniques are introduced to perform a sensitivity analysis for mercury over Europe, using a regional model. This approach differs from other techniques such as the direct and indirect approaches developed to compute sensitivities for air quality modeling. Gaseous elemental mercury life-time being of order one year, global or hemispherical models are usually preferred to analyze its fate and transport. In an area limited domain, respective influence of incoming mercury and inner emissions fluxes have to be weighted. A local measurement depends on the potential ground emissions, the potential incoming mass from domain borders and on the potential initial content in mercury of the atmosphere. The sensitivities of the measurement to entire maps of emissions, boundary conditions, etc., are computed thanks to the adjoint method since other techniques do not allow to perform these computations directly. As an application to this methodological developments, we use the numerical transport model Polair3D. Quantitative sensitivity maps are provided for EMEP mercury monitoring stations. With the adjoint approach, sensitivities of a given country to other countries emissions are computed in a straightforward manner. The yearly average sensitivity of a measurement of gaseous elemental mercury to distant sources is shown to decrease like a power law $r^{-2.4}$, where r is the distance to a source. It is eventually explained how the method developed here can be generalized to account for a more complex mercury chemistry, and the modeling of oxidized species. In particular sensitivities of dry and wet deposition fluxes of oxidized species are computed for one EMEP station.

1. Introduction

Several Chemistry Transport Models (CTM) are currently used to simulate atmospheric mercury dispersion. Since mercury is considered as a global pollutant, due to its relative long atmospheric life time of about one year, most of them run on a global domain (Seigneur et al. [2001]) or a hemispherical one (Ilyin et al. [2002], Christensen et al. [2004]). Such models proved well suited to the study of transboundary pollution. They also provide boundary conditions for regional models. The latter are suitable for impact studies needing finer spatial resolution, global model having too coarse resolution to get accurate estimations of deposition fluxes. Some simulations are still performed within a restricted domain (Lin and Tao [2003], Bullock and Brehme [2002]). They generally stand as a first step in atmospheric mercury model development, to assess qualitatively the impact of new reaction kinetics or to highlight an improved parameterization of a physical process.

The first aim of this work is to assess some strength and limitations of atmospheric mercury modeling when using a regional model. Europe will be studied as an open system, subject to external influences, encapsulated in the boundary conditions, and to internal influences : sources, sinks, initial bulk concentration levels. Such a study can be performed from a quantitative point of view through a sensitivity analysis. First sensitivity studies focussing on the transport and fate of mercury within a regional model were performed in (Pai et al. [1999]; Xu et al. [2000]). The authors have made use of the indirect technique (single perturbation, or brute-force method). Their conclusions point out to the most sensitive parameters regarding mercury deposition such as speciation of emissions, dry deposition parameterization, oxidizing species ambient concentrations, etc. In this paper, we will be mainly interested in sensitivities to parameters which are crucial to regional modeling of mercury air concentrations. For instance, one should evaluate the influence of boundary conditions on a measurement, as compared to inner sources of mercury. We will also be interested in sensitivities to initial conditions, inner sources and emissions. Typical questions to be answered are : what is the annual average influence of westerly incoming mercury on a local concentration measurement, compared to the regional emissions influence? Another typical issue is to assess the potential influence (knowing the meteorological conditions) of European emissions on the concentrations over a given country. Note that it is quite a different question from knowing the influence one country emissions have on the rest of Europe. This last question would be directly addressed by other known methods.

In this respect, the second aim of this work is to develop the appropriate techniques to compute those sensitivities. Several techniques have been developed for air quality models to study sensitivities. The Decoupled Direct Method [DDM] (Dunker et al. [2002] and references therein) is a robust technique. It consists in exploiting the exact numerical scheme which simulates the propagation of a perturbation though the original numerical model. A variant is to carry out this program systematically using automatic differentiation (Carmichael et al. [1997]). The indirect method studies the propagation of a perturbation in the parameters, possibly using finite differences. This technique has been used in the study of the fate and transport of mercury (Pai et al. [1999]). These methods made use of the forward model, or of its formal derivative. In all cases, the forward propagation of a perturbation is studied. A quite different point of view focusses on the adjoint model (Uliasz [1983]; Daescu and Carmichael [2003]). In that case, the perturbation is propagated backward from the observation station to the area mostly contributing to the measurement at the station. This is known as the adjoint method, and in another form Green function method (Vuillemier [1997]).

The technique we would like to advocate belongs to the class of adjoint methods. It relies on the linearity in the species concentrations of the models of mercury transport and fate. Because of this property, some simplifications to the adjoint variational methods used in air quality models (Elbern [1999]) focussing on photo-chemistry are operated. Such an approach has been emphasized in (Uliasz [1983]; Marchuk [1995]). A similar approach has been used for CO_2 inverse modeling (Kaminski et al. [1999]) through the technique of the Jacobian (actually equivalent to the method we

advocate). However it was formulated for a global domain. The adjoint analysis in presence of boundaries is somewhat more intricate (Uliasz [1983]). A recent work (Cosme et al. [2005]) has applied those techniques to the investigation of origin of sulfur compounds detected in Eastern Antarctica.

The method we develop in this paper has advantages over previously used sensitivity analysis techniques. First, thanks to the linearity assumption, adjoint solutions which synthesize all first-oder sensitivities can be computed once and for all. As a consequence, various analysis can later be performed quickly and efficiently on a single PC, using the stored adjoint solutions. Second, because of the backward point of view (specific to adjoint methods), quantitative results such as sensitivities of measurement or an average measurement over a large area (such as a country) with respect to emissions, boundary conditions, etc, can be obtained in a single run. Forward methods (both direct and indirect) are not as straightforward (Ilyin et al. [2003]).

To emphasize the advantages of the method, it will be applied on several mercury sensitivity problems. The method stands as an alternate way to establish source-receptor relationships, focussing on the receptor as a starting point of the computation, instead of the sources (Seigneur et al. [2004]). Sensitivity of a measurement at a given receptor to all domain sources (and mercury species) will be computed in a single run of the adjoint model. As another application building on the previous one, the average influence of sources on a station will be computed in terms of the source-receptor distance. The adjoint techniques will be shown to help quantify the mercury budget within the limits of a regional model. Regional modeling of mercury transport should benefit from that analysis.

In section 2 of this paper, the mercury dispersion model used to exemplify the method is detailed. In section 3, the way adjoint methods should be used to study open systems is advocated, both for the continuous and the numerical (discrete) models. In section 4, it is shown how these developments help carrying out a quantitative sensitivity analysis and first results on mercury over Europe are exposed. In section 5, the methodology is generalized to a more complex chemistry accounting for oxidized species and an application is given. Conclusions are given in section 6.

2. Simulating mercury over Europe

The transport and fate of mercury is governed by the equation :

$$\frac{\partial c}{\partial t} + \operatorname{div}(\boldsymbol{u}c) - \operatorname{div}(\boldsymbol{K}\nabla c) + \Lambda\, c = \sigma\,. \tag{1}$$

It describes the temporal evolution of mercury concentration $\frac{\partial c}{\partial t}$, under the influence of the following processes :

- the advection by wind $\boldsymbol{u}$, $\operatorname{div}(\boldsymbol{u}c)$,
- the turbulent diffusion term with $\boldsymbol{K}$ the eddy diffusivity tensor, $\operatorname{div}(\boldsymbol{K}\nabla c)$,
- the chemistry and wet scavenging process are altogether described by $\Lambda\, c$,
- and the volume emission term, σ.

Another important physical process is the dry deposition, enforced here as a boundary condition :

$$(\boldsymbol{K}\nabla c)\cdot\boldsymbol{n} = E - v^{\mathrm{dep}}\, c\,, \tag{2}$$

with the normal surface vector $\boldsymbol{n}$, outward oriented, the ground emission term E and the dry deposition term $v^{\mathrm{dep}}\, c$ (v_d is the dry deposition velocity). Λ and v^{dep} depend specifically on mercury-related physical parameterizations.

2.1. Physical parameterizations

Mercury can be found under multiple forms in the atmosphere, elemental mercury, Hg(0), representing by far the dominant one in mass (95-99 %, (Ryaboshapko et al. [2002])). Oxidized or divalent mercury species also exist, carried by atmospheric particle (HgP) or not (Hg(II)). Mercury under all these forms is present in both gaseous and aqueous phases. Residence times in the atmosphere of mercury species vary between one year for gaseous elemental mercury [GEM] (Lindqvist and Rodhe [1985]), days to weeks for particulate mercury and hours to days for oxidized species (Seigneur et al. [2003]). Life time of mercury species are related to their physical and chemical properties that largely influence their rates of dry and wet deposition (Schroeder and Munthe [1998]). Consequently to its long life time GEM is well mixed in the atmosphere, concentration fields are quite homogeneous with typical values in the range of one to two $\mathrm{ng.m^{-3}}$. With modeling issues in mind, this behavior suggests that boundary conditions for a regional model are rather influential.

Although GEM has a low reactivity and solubility, one should take into account its possible chemical and physical transformations into oxidized mercury species, which are much more soluble and hence likely to be quickly deposited. Gaseous oxidation rates of mercury are quite weak over Europe, either because reaction kinetics are relatively slow (with O_3 for example, Hall [1995]) or the oxidant species concentrations are low (it is the case with hydroxyl radicals, Sommar et al. [2001]). However fast mercury depletion events (MDE) occur over polar regions. These MDE, involving molecular and atomic halogens, are currently addressed in several works (see Ariya et al. [2004] and references therein). Since Arctic, and more precisely marine frozen area, do not represent an appreciable part of our regional domain, these fast processes in gaseous phase are not treated. In aqueous phase reactions implying mercury species may have fast kinetics. Oxidized mercury species in aqueous phase can be adsorbed by particulate matter to form particulate mercury.

Two mercury chemistry models have been implemented in the model we use in this work : Polair3D (Sportisse et al. [2002]; Sartelet et al. [2002]; Boutahar et al. [2004]). The first one is a simple model allowing to simulate mercury chemical behavior through a scavenging ratio (Petersen et al. [1995]). Only one transport equation for GEM is resolved. Forced concentration fields are used for O_3 and particulate matter to determine the scavenging ratio obtained with several equilibria hypothesis and consideration on concentrations magnitude. An interesting point is that the chemistry-scavenging term in Eq.(1) as the other ones is linear. In practice, numerically modeled GEM nearly behaves like a passive tracer because scavenging coefficients are quite low. The second, conceived on the basis of more complex models (Ryaboshapko et al. [2002]), represents several mercury species interacting in gaseous and aqueous phases. Simulations for the year 2001 have been performed with both models and results compare well with the available EMEP measurements for air concentrations (Roustan et al. [2005]).

In section 3 and 4, the sensitivity analysis is focussed on GEM concentrations. Its simulation only necessitates the simplified model. In currently developed models, a more complex chemistry allows for a more precise evaluation of oxidized species concentration fields and therefore better deposition flux patterns. The second model will be used in section 5 to obtain sensitivity of the depositions fluxes with respect to oxidized species.

Two different removal mechanisms of pollutants from the atmosphere are usually considered : wet and dry deposition. In the case of mercury these processes are known to be the

main pathways from the atmosphere to biological organisms, especially in the aquatic food chain.

Usually dry deposition represents three consecutive processes that bring pollutant from the atmosphere to soil surface under dry conditions (Wesely and Hicks [2000]). Turbulent diffusion is the dominant process taking place in most of the layer between the reference height where dry deposition velocity is estimated, and the soil. Gaseous molecular diffusion becomes the major process in the last millimeters corresponding to quasi-laminar layer. The mass transfer process from the air to the canopy (absorption/adsorption by vegetals or surface water, etc) completes the removal mechanism. Each step of the transfer is represented by a deposition resistance, the inverse of the sum of the resistances being the dry deposition velocity. The pollutant dry deposition flux is given by the product of pollutant concentrations by the dry deposition velocity. For current simulations a big-leaf model is used, i.e. the canopy is treated as a single leaf without taking into account its vertical structure, which would be done by multi-layer model. Resistances parameterization are inspired by (Baer and Nester [1992]) with some improvements, in particular for the quasi-laminar boundary resistance over sea (Hicks and Liss [1976]) and the canopy water content consideration in canopy resistance (Brook et al. [1999]). Those parameterizations are further detailed in (Roustan et al. [2005]).

Wet deposition can be split into two phenomena, in-cloud scavenging and below cloud scavenging. In-cloud scavenging deposition results from pollutant mass transfer into cloud drops followed by transport to the surface during precipitation events. The mass transfer can be treated by the chemistry model with Henry equilibrium hypothesis or using kinetic consideration if the equilibrium state is not reached. The mass removed by rain is estimated with a scavenging coefficient depending on rain intensity and cloud liquid water content. Below cloud scavenging represents effects of falling rain drops on pollutant in the atmosphere, here again a scavenging coefficient is used to determine the deposition flux. Obviously the impact of these two phenomena depend on pollutant solubility and precipitation intensity. As said previously, the simple model take into account the chemical processes through a scavenging ratio. Instantaneous Henry equilibrium hypothesis is used due to the low solubility of Hg(0). Aqueous species are not explicitly simulated. For these reasons it may be more appropriate to speak here simply about wet scavenging rather than below and in-cloud scavenging. For the complex model used in section 5, both processes are distinctively treated. The below cloud scavenging is determined using the parameterization studied in (Sportisse and du Bois [2002]). The chemistry model deals with the mass transfer between gaseous and aqueous phase and the scavenging coefficient is determined according to (Roselle and Binkowski [1999]).

2.2. A regional model

The transport and physics of mercury is meant here to be simulated over Europe. The domain which is considered (Fig.1) extends in space from 12.375° W to 37.125° E in longitude and from 36° N to 72° N in latitude. One to five years of mercury dispersion are simulated. Direct and backward simulations are mainly performed for the year 2001. A constant grid resolution of 1.125° is taken along longitude and latitude for the grid of 44×32 cells respectively. The 14 vertical levels, defined in a z-coordinate system, cover the lower troposphere from the ground to 5233 m in relative height.

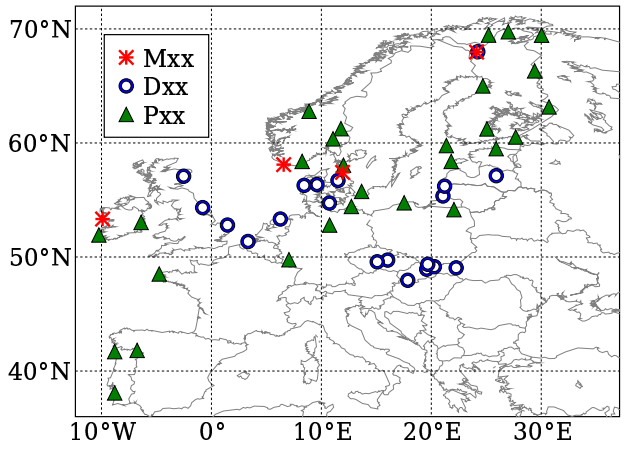

Figure 1. Representation of the domain $\mathcal{D}$. Symbols $*$, $\circ$, and $\blacktriangle$ indicate gaseous mercury stations, gaseous heavy metal stations, and precipitation stations respectively.

The domain is designated by Ω and it is the product of its spatial and temporal components $\Omega = \mathcal{D} \times [0, \tau]$. The boundaries of the domain Ω are denoted $\partial\Omega_0$, $\partial\Omega_\tau$, $\partial\Omega_b$, $\partial\Omega_t$, $\partial\Omega_n$, $\partial\Omega_s$, $\partial\Omega_w$ and $\partial\Omega_e$, for respectively the initial, final, surface, top, North, South, West and East boundaries. The boundary of the space domain is denoted $\partial\mathcal{D}$. A distinction is to be made between border interfaces where the wind is incoming, and border interfaces where it is outgoing. Hence the spatial boundary splits into $\partial\mathcal{D} = \partial\mathcal{D}_+ \cup \partial\mathcal{D}_-$ ($+$ means incoming, and $-$ means outgoing). Note that this decomposition is time-dependent. We will also denote $\partial\Omega_\pm = \bigcup_t \partial\mathcal{D}_\pm[t]$. Finally, $\partial\mathcal{D}$, the spatial boundary of $\mathcal{D}$, is made up of the bottom (surface), top, North, South, West and East borders, $\partial\mathcal{D}_b$, $\partial\mathcal{D}_t$, $\partial\mathcal{D}_n$, $\partial\mathcal{D}_s$, $\mathcal{D}_w$, and $\partial\mathcal{D}_e$ respectively.

To support some of our results, forward simulations will be performed. However, the actual boundary condition values used in those simulations are secondary. Since the transport and fate of mercury is linear, sensitivities do not depend on them. For these simulations the following boundary conditions are implemented : 1.75 ng.m^{-3} at West, 1.7 ng.m^{-3} at East, 1.5 ng.m^{-3} at South and 1.42 ng.m^{-3} at North. These values are proposed by the Meteorological Synthesizing Centre - East (MSC-E) in a first approach (`http://www.msceast.org/`). In addition a value of 1.6 ng.m^{-3} at the top of the domain was chosen. The relevance of these choices are discussed in (Roustan and Bocquet [2005]). However, the precise values do not have any consequence on the sensitivity analysis carried out in this paper.

3. Adjoint transport in an open domain

Adjoint analytical and numerical techniques will now be applied to the study of mercury concentration sensitivity in the framework of a European dispersion model.

3.1. Continuous analysis

Consider the transport equation Eq.(1). It may be multiplied against a test function ϕ defined on the whole space-

time domain Ω :

$$\int_\Omega \mathrm{d}t\mathrm{d}\boldsymbol{x}\,\phi\quad\frac{\partial c}{\partial t}+\mathrm{div}\,(\boldsymbol{u}c)-\mathrm{div}\,(\boldsymbol{K}\nabla c)+\Lambda\,c-\sigma\quad=0\,. \tag{3}$$

ϕ is assumed sufficiently regular for the integrals to be properly defined. The first term can readily be transformed into

$$\begin{aligned}\int_\Omega \mathrm{d}t\mathrm{d}\boldsymbol{x}\,\phi\frac{\partial c}{\partial t}=&-\int_\Omega \mathrm{d}t\mathrm{d}\boldsymbol{x}\,c\frac{\partial \phi}{\partial t}\\&+\int_{\mathcal{D}}\mathrm{d}\boldsymbol{x}\;[c(\tau)\phi(\tau)-c(0)\phi(0)]\;.\end{aligned} \tag{4}$$

Using the continuity equation for an incompressible fluid $\mathrm{div}(\boldsymbol{u})=0$ (an assumption which is consistent with Eq.(1), but not necessary to the derivation of an adjoint), the advection term can be transformed into

$$\begin{aligned}\int_\Omega \mathrm{d}t\mathrm{d}\boldsymbol{x}\,\phi\,\mathrm{div}\,(\boldsymbol{u}c)=&-\int_\Omega \mathrm{d}t\mathrm{d}\boldsymbol{x}\,c\,\mathrm{div}\,(\boldsymbol{u}\phi)\\&+\int_{\partial\mathcal{D}\times[0,\tau]}\mathrm{d}t\mathrm{d}\boldsymbol{S}\cdot(\phi c\boldsymbol{u})\;.\end{aligned} \tag{5}$$

As for the diffusion term, one gets

$$\begin{aligned}\int_\Omega \mathrm{d}t\mathrm{d}\boldsymbol{x}\,\phi\,\mathrm{div}\,(\boldsymbol{K}\nabla c)=&\int_\Omega \mathrm{d}t\mathrm{d}\boldsymbol{x}\,c\,\mathrm{div}\,(\boldsymbol{K}\nabla\phi)\\&+\int_{\partial\mathcal{D}\times[0,\tau]}\mathrm{d}t\mathrm{d}\boldsymbol{S}\cdot(\phi\boldsymbol{K}\nabla c-c\boldsymbol{K}\nabla\phi)\end{aligned} \tag{6}$$

Gathering these terms, one obtains

$$\begin{aligned}0=&\int_\Omega \mathrm{d}t\mathrm{d}\boldsymbol{x}\,c\quad-\frac{\partial\phi}{\partial t}-\mathrm{div}\,(\boldsymbol{u}\phi)-\mathrm{div}\,(\boldsymbol{K}\nabla\phi)+\Lambda\,\phi\\&-\int_\Omega \mathrm{d}t\mathrm{d}\boldsymbol{x}\,\phi\,\sigma+\int_{\mathcal{D}}\mathrm{d}\boldsymbol{x}\;[c(\tau)\phi(\tau)-c(0)\phi(0)]\\&+\int_{\partial\mathcal{D}\times[0,\tau]}\mathrm{d}t\mathrm{d}\boldsymbol{S}\cdot(c\boldsymbol{K}\nabla\phi-\phi\boldsymbol{K}\nabla c)\\&+\int_{\partial\mathcal{D}\times[0,\tau]}\mathrm{d}t\mathrm{d}\boldsymbol{S}\cdot(\phi c\boldsymbol{u})\;.\end{aligned} \tag{7}$$

This identity is valid for any test function ϕ. Our goal is to make a choice for ϕ, which allows to connect modelled measurements to the inputs of the model (sources, emissions, transboundary transport), in the most convenient way. First, we would like the first integral to represent a concentration measurement. This measurement (of value μ_i, performed on site i) is completely characterized by a sampling function $\pi_i:\Omega\to\mathbb{R}$, such that $\int_\Omega \mathrm{d}t\mathrm{d}\boldsymbol{x}\,\pi_i(\boldsymbol{x},t)=1$ and

$$\mu_i=\int_\Omega \mathrm{d}t\mathrm{d}\boldsymbol{x}\,\pi_i(\boldsymbol{x},t)\,c(\boldsymbol{x},t)\,. \tag{8}$$

It is therefore natural to require for ϕ, which we shall denote from now on c_i^*, to be a solution of the retro-transport equation

$$-\frac{\partial c_i^*}{\partial t}-\mathrm{div}\,(\boldsymbol{u}c_i^*)-\mathrm{div}\,(\boldsymbol{K}\nabla c_i^*)+\Lambda c_i^*=\pi_i\,. \tag{9}$$

To characterize c_i^* completely, boundary and initial conditions must be specified. As is clearly seen from Eq.(9), the adjoint solution c_i^* corresponds to a transport backward in time. However it is not the reverse of the direct model solution. The wind field is the opposite of the direct model wind-field. As a consequence, an outgoing (from the domain $\mathcal{D}$) wind flow for the direct model is actually an incoming wind flow for the adjoint model. In order to specify the incoming mercury, one therefore needs to specify its concentration on $\partial\mathcal{D}_-$ at any time. For simplicity,

$$\forall\,(\boldsymbol{x},t)\in\partial\Omega_-\,,\quad c_i^*(\boldsymbol{x},t)=0\,, \tag{10}$$

is assumed (among other possible choices). This reduces the last integral of Eq.(7) from an integral over $\partial\mathcal{D}\times[0,\tau]$ to an integral over $\partial\Omega_+$.

In addition, the diffusive fluxes $-\boldsymbol{K}\nabla c$ and $-\boldsymbol{K}\nabla c_i^*$ at the top and lateral boundaries $\partial\mathcal{D}$ are taken to be null. However at the surface, $-\boldsymbol{K}\nabla c$ is no different than the surface emission $\boldsymbol{J}$. In a similar fashion, $-\boldsymbol{K}\nabla c_i^*$ is given a value $\boldsymbol{J}_i^*$ at the surface which is to be prescribed later on.

Finally, the adjoint concentration field c_i^* is set to be null at initial time, which is $t=\tau$ (simplest choice over many possible).

Eventually, one obtains for this almost completely specified adjoint solution

$$\begin{aligned}\mu_i=&\int_\Omega \mathrm{d}t\mathrm{d}\boldsymbol{x}\,c_i^*\,\sigma+\int_{\partial\Omega_0}\mathrm{d}\boldsymbol{x}\,c_i^*\,c\\&+\int_{\partial\Omega_b}\mathrm{d}t\mathrm{d}\boldsymbol{S}\cdot(c\,\boldsymbol{J}_i^*-c_i^*\,\boldsymbol{J})-\int_{\partial\Omega_+}\mathrm{d}t\mathrm{d}\boldsymbol{S}\cdot(c_i^*c\boldsymbol{u})\;.\end{aligned} \tag{11}$$

As for $\boldsymbol{J}_i^*$, the simplest choice would be to take it null. Let us denote $\boldsymbol{n}$ the unit vector orthogonal to the boundary, oriented outward ($\mathrm{d}\boldsymbol{S}=\mathrm{d}S\,\boldsymbol{n}$). In Polair3D, $\boldsymbol{J}\cdot\boldsymbol{n}$ stands actually for $v^{\mathrm{dep}}c_{|b}-E$. That is why the choice $\boldsymbol{J}_i^*\cdot\boldsymbol{n}=v^{\mathrm{dep}}c_{i\,|b}^*$ allows for a simplification in the kernel :

$$\int_{\partial\Omega_b}\mathrm{d}t\mathrm{d}\boldsymbol{S}\cdot(c\,\boldsymbol{J}_i^*-c_i^*\,\boldsymbol{J})\to-\int_{\partial\Omega_b}\mathrm{d}t\mathrm{d}\boldsymbol{S}\cdot(c_i^*\,\boldsymbol{E})\;, \tag{12}$$

with $\boldsymbol{E}=-E\,\boldsymbol{n}$. Therefore this specific choice of the adjoint solution makes the connection between the output and the surface emission clearer. This choice of adjoint solution stipulates dry deposition is to be taken into account in the calculation of the retroplume.

Formula (11) makes a clear connection between inputs ($\boldsymbol{J}$, σ, c on $\partial\Omega_+$, c on $\partial\Omega_0$, possibly c on $\partial\Omega_b$) and the output (μ_i). The adjoint solution stands as a kernel characterizing the linear operator making the connection. Once the adjoint solution is stored, the output can easily be calculated from any set of input. When obtaining sensitivities to emissions, ground sources, boundary conditions, only slices of the retroplume on the boundaries need to be stored.

3.2. Application to a numerical transport model

The analysis performed above is based on a continuous modeling. However to perform numerical calculations with a dispersion model, an analog analysis should be carried out for the numerical model. The dual analysis we have done which led to continuous adjoint solutions should be carried over to the discrete case. However, this is not straightforward (see the discussion of Hourdin et al. [2005] in the case of a passive tracer).

The domain Ω is discretized into a grid (seen as a set of cells) $\overline{\Omega}=\bigcup_k\Omega_k$, where Ω_k is a grid-cell. k is the running index of the (space and time) discretization mesh. A border cell belongs to one of the grid boundaries $\overline{\partial\Omega}_0$, $\overline{\partial\Omega}_\tau$, $\overline{\partial\Omega}_b$, $\overline{\partial\Omega}_t$, $\overline{\partial\Omega}_n$, $\overline{\partial\Omega}_s$, $\overline{\partial\Omega}_w$ and $\overline{\partial\Omega}_e$. Boundaries $\overline{\partial\Omega}_\pm$ are the grid cells forming the one layer boundary of $\overline{\Omega}$, discretized analog of $\partial\Omega_\pm$.

In this paper, we will apply our methods using the Chemistry Transport Model Polair3D ((Sportisse et al. [2002]; Sartelet et al. [2002]; Boutahar et al. [2004]; Roustan et al. [2005])). The numerical code is based on a first order time splitting algorithm allowing to separate temporally chemistry (when relevant), advection and diffusion. The advection scheme is a third-order Direct Space Time

(DST) scheme (Spee [1998]) with the Koren-Sweby flux limiter function. Its related temporal scheme is explicit. The diffusion scheme is a spatially centered three-point scheme. Its related temporal scheme is a semi-implicit Rosenbrock scheme. As a consequence, there is no simple closed discrete equation analog to the continuous transport Eq.(1). So there is no obvious dual treatment, which would lead explicitly to the adjoint numerical code (not to mention possible non-linearity in the advection scheme). POLAIR3D was however coded in such a way that it can be automatically differentiated and its adjoint obtained (Mallet and Sportisse [2004]).

Still, we intend to go further without resorting to automatic differentiation. The spatial discretization schemes are not problematic since there are explicit. Taking the adjoint of the time discretization is more intricate. Actually the first-order splitting is time-symmetric by construction, so that the adjoint numerical code is also in the form of a first-order splitting. The time discretization of advection being explicit, the time-reversal operation is an easy task and leads to an equivalent explicit scheme. The time diffusion scheme being a Rosenbrock semi-implicit scheme, the time-symmetry is slightly broken, but only because K_z is time-dependent (though linear, the eddy-diffusion operator is not constant). Therefore it appears that, in its linear regime, POLAIR3D is almost time-symmetric. It can be shown that (still in its linear regime) the bulk part of POLAIR3D is space-symmetric for the eddy-diffusion part and space-antisymmetric for the advection scheme. Detailed calculations show that the adjoint of POLAIR3D would be POLAIR3D itself, antisymmetric fields such as wind fields being reversed, if not for occasional non-linearity and if not the K_z time-dependence. As a conclusion, the numerical model can be used to simulate adjoint solutions, using the specific of the adjoint equation (backward in time, wind fields reversed, kinetic matrix transposed). This provides with an efficient method to calculate approximate adjoint solutions.

The calculations not only yield the bulk term of the adjoint numerical schemes, but also the boundary terms, which are crucial to our analysis.

We can summarize the results of those calculations with the formula :

$$\begin{aligned}\mu_i = &\sum_{k\in\overline{\Omega}} c^*_{i,k}\,\sigma_k + \sum_{k\in\overline{\partial\Omega}_0} c^*_{i,k}c_k \\ &+ \sum_{k\in\overline{\partial\Omega}_b} c^*_{i,k}J_k - c_k J^*_{i,k} \;+ \sum_{k\in\overline{\partial\Omega}_+} c^*_{i,k}F_k\,,\end{aligned} \tag{13}$$

very similar to its continuous counterpart. Space and time volume elements which appear in the discretized sums have been integrated into the sources σ_k, space volume elements have been integrated into the initial concentrations $c_{k\,|0}$, whereas surface elements have been integrated into the emissions $J^*_{i,k} = -\boldsymbol{n}\cdot\boldsymbol{F}^*_{i,k}$ and $J_k = -\boldsymbol{n}\cdot\boldsymbol{J}_k$, and the advection fluxes $F_k = -\boldsymbol{n}\cdot\boldsymbol{F}_k$. Therefore, they are all expressed in units of mass. The numerical advection flux F_k could be specified precisely in terms of boundary concentrations and wind fields, with the details of the adjoint calculations. It is positive by definition on $\partial\Omega_+$.

In the case where $\boldsymbol{J}^*_i\cdot\boldsymbol{n} = v^{\mathrm{dep}}c^*_{i\,|b}$, Eq.(13) simplifies to

$$\begin{aligned}\mu_i = &\sum_{k\in\overline{\Omega}} c^*_{i,k}\,\sigma_k + \sum_{k\in\overline{\partial\Omega}_0} c^*_{i,k}c_k \\ &+ \sum_{k\in\overline{\partial\Omega}_b} c^*_{i,k}E_k + \sum_{k\in\overline{\partial\Omega}_+} c^*_{i,k}F_k\,.\end{aligned} \tag{14}$$

As explained before, several mild approximations are used to compute adjoint solutions. In the next section, the validity of this approximation will be tested. It incidentally exemplifies a few differences between a forward approach to calculate sensitivities (direct and indirect methods) and the adjoint approach.

3.3. Matching the forward and adjoint approaches

Formula (14) has decomposed a concentration measurement in terms of contributions from sources, from ground emissions, from incoming fluxes, which multiply parts of the adjoint solution. On the other hand, the direct formula (using forward simulations) for the same measurement reads

$$\mu_i = \sum_{k\in\overline{\Omega}} \pi_{i,k}\,c_k\,. \tag{15}$$

Owning to superposition principle (because of the linearity of the model), the components of μ_i ascribable to the sources, incoming fluxes, etc, are computed in a forward simulation by shutting off all contributions but the one studied (single perturbation). A comparison can then be established between the components of μ_i computed by simulation and those calculated by the adjoint technique. If the numerical solution c^*_i was a perfect adjoint solution to the concentration field c, then one should expect Eq.(14) and Eq.(15) to yield exactly the same result within numerical roundoff errors. So would one for the separate contributions to μ_i. However, due to the approximations used, this should not necessarily be so. Nevertheless, the discrepancy should be small. This discrepancy is both a test for the approximations made in the computation of the adjoint solution and when taking the numerical model to be linear.

Such a test was performed for a set of stations for year 2001. $p = 52$ sites have been chosen to perform adjoint simulations. They correspond to measurement stations belonging to the EMEP network in charge of the heavy metals monitoring (Aas and Hjellbrekke [2003]). The first four are devoted to the observation of mercury air concentrations (Mxx). The next twenty (Pxx) are originally intended for the air concentrations measurement of other heavy metals (for example lead and cadmium). The last twenty-eight (Dxx) correspond to survey stations for concentration in precipitation. Since some stations are equipped for both air and water measurements, they are not used twice. The stations sites have been plotted in Fig.1.

We have estimated statistically the error committed between the direct and the indirect calculations of the measurements μ_i. The bias is 0.05 ng.m^{-3}, the fractional bias is 2.3 %, the normalized root mean square is 2.8 %, and the individually normalized root mean square (in that case, the normalization is not global but for each measurement discrepancy) is 2.3 % (see appendix A for a proper definition). We consider these errors to be acceptable for the following sensitivity analysis. As for the errors due to small non-linearities (advection scheme, possibly clipping of concentrations), the differences between a multiple single-components runs and a single multiple-component runs have been checked. This tests the additivity principle. The difference is negligible with a maximum not exceeding 0.5 %. So that the non-linearity introduced to numerically model linear processes is not an issue.

This test is yielding byproducts concerning the relative contributions of mercury sources, incoming fluxes, initial state, to observations. Below are given four examples of stations. The first two are drawn from the four European GEM stations mentioned here : the first one is located at Mace Head (Ireland) (IE31 in the EMEP nomenclature), very close to the North-West corner of the domain, the second one is in Pallas (Finland) (FI96), North-East of the domain. Both are strongly influenced by boundary conditions, and little by European emissions, in particular the

anthropogenic ones. The next two stations are observation stations for cadmium and lead. They are given as examples because of their central location : Deuselbach (Germany) (DE04) and Topolniky (Slovakia) (SK07), where we expect European emissions to be much more influential.

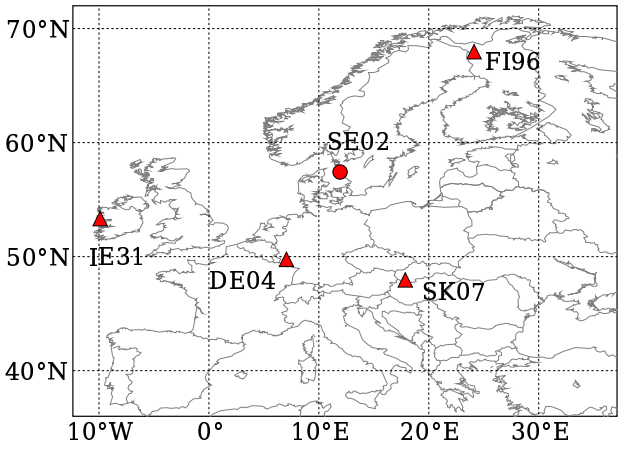

Figure 2. Locations of the four stations described in section 3.3 (▲) and location of the station used for applications in sections 4.4 and 5.3 (●).

Results are compiled in table 1.

3.4. Contributions at a receptor

For off-center stations, European emission direct contribution is limited to a few percents, whereas for central stations it is up to 30%. By direct contribution it is intended that the measurement incorporates contribution from trajectories that remain within the domain Ω. There are however trajectories that go out of the domain, come in later and eventually reach the station to contribute to the measurement. Those are not taken into account directly but hopefully through the undifferentiated incoming advected mercury (see Fig. 3).

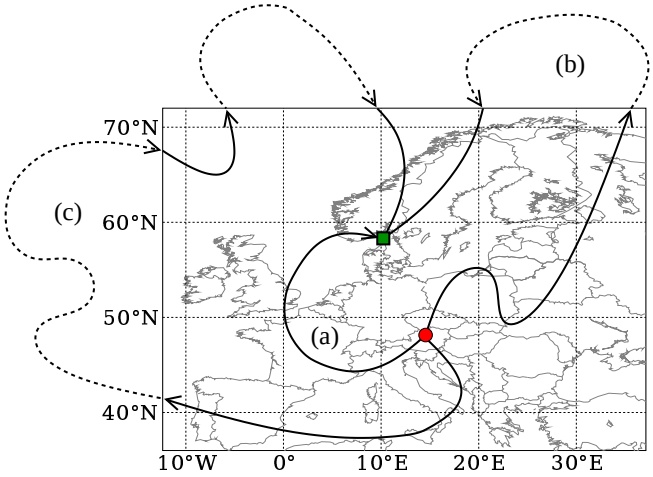

Figure 3. Possible trajectories for a mercury particle from the emitter (disk) to the monitoring station (square). Those coming out, then in, (b,c) are not accounted for in the emission contribution but rather in the incoming mercury flux, contrary to inside trajectories (a).

This is one limitation, though well circumvented, of the limited-domain approach. Therefore 30% must be understood as a lower bound for the European contribution to (re-)emissions.

Table 1. Contribution to GEM concentrations in ng.m^{-3} for year 2001 over Europe, as computed from direct simulations (right), and from adjoint simulations (left).

Station	Winds	Emissions	Total
Mace Head IE31	1.735 - 1.717	0.163 - 0.137	1.901 - 1.856
Pallas FI96	1.582 - 1.541	0.088 - 0.086	1.670 - 1.625
Deuselbach DE04	1.690 - 1.647	0.875 - 0.819	2.565 - 2.469
Topolniky SK07	1.665 - 1.641	1.092 - 1.061	2.757 - 2.708

4. First-order sensitivity analysis using the adjoint method

The source-receptor method tells what impact an emitting region has on the other regions. It requires a direct simulation (forward model). Such an analysis is possible because the transport and chemistry of mercury are linear or more accurately considered so. Indeed this allows a region to be studied independently of the others. Then the additivity principle applies. Single perturbation techniques and the DDM method are appropriate for these studies.

4.1. Adjoint solutions and sensitivities

However it is quite a different question to know what effects emissions from the rest of the world have on a region. It raises the question of the sensitivity of the region with

respect to emissions from itself and/or other regions. It requires a backward simulation but also relies on the linearity hypothesis.

4.1.1. Extracting the sensitivities

Formally, sensitivities are given by the functional partial derivative of the measurement (μ_i is the concentration level of the local grid-cell region) with respect to local fields. What can be learnt from Eq.(11) is

$$\begin{aligned} &\frac{\delta\mu_i}{\delta\sigma} = c_i^* \,, \qquad \frac{\delta\mu_i}{\delta c_{|0}} = c_{i\,|0}^* \,, \qquad \frac{\delta\mu_i}{\delta(\boldsymbol{J}\cdot\boldsymbol{n})} = -c_{i\,|b}^* \,, \\ &\frac{\delta\mu_i}{\delta c_{|b}} = \boldsymbol{J}_i^*\cdot\boldsymbol{n} \,, \qquad \frac{\delta\mu_i}{\delta c_{|+}} = -\left(c_i^*\boldsymbol{u}\right)_{|+}\cdot\boldsymbol{n} \,. \end{aligned} \tag{16}$$

where $J = \boldsymbol{J}\cdot\boldsymbol{n}$. $+$ and $-$ are referring to incoming and outgoing boundaries. 0 and b are referring to initial state and surface state.

4.1.2. Average sensitivity

The adjoint solution pieces can be represented by very large fields. In some cases they depend on position and time. To represent them graphically, one therefore needs moments of the field, such as the temporal mean. Sensitivity to emissions can therefore be investigated through its temporal mean on a 2D map. However the meaning of an averaged sensitivity is not obvious. For the demonstration, assume the emission field $\boldsymbol{E}(\boldsymbol{x},t)$ is constant in time. Then the measurement equation reads

$$\mu_i = -\int_{\partial\Omega_b} \mathrm{d}t\mathrm{d}\boldsymbol{S}\cdot\left(c_i^*(\boldsymbol{x},t)\,\boldsymbol{E}(\boldsymbol{x})\right) + \cdots \tag{17}$$

$$= -\int_{\partial\Omega_b} \mathrm{d}\boldsymbol{S}\cdot\boldsymbol{E}(\boldsymbol{x}) \int_{[0,\tau]} \mathrm{d}t\, c_i^*(\boldsymbol{x},t) + \cdots \,. \tag{18}$$

As a consequence,

$$\frac{\delta\mu_i}{\delta E(\boldsymbol{x})} = \int_{[0,\tau]} \mathrm{d}t\, c_{i\,|b}^*(\boldsymbol{x},t) \,, \tag{19}$$

and the time-averaged sensitivity to emissions can be interpreted as the sensitivity to a time-independent emission field.

4.1.3. Numerical sensitivities

As for the numerical model, the sensitivities are

$$\begin{aligned} &\frac{\delta\mu_i}{\delta\sigma_k} = c_{i,k}^* \,, \qquad \frac{\delta\mu_i}{\delta\left(c_k\right)_{|0}} = c_{i,k\;|0}^* \,, \qquad \frac{\delta\mu_i}{\delta E_k} = c_{i,k\;|b}^* \,, \\ &\frac{\delta\mu_i}{\delta\left(c_k\right)_{|b}} = -J_{i,k}^* \,, \qquad \frac{\delta\mu_i}{\delta F_k} = c_{i,k\;|+}^* \,, \end{aligned} \tag{20}$$

which is derived from Eq.(14). Those sensitivities are not independent from one another. Moreover they are complete, which means that measurements at site i are fully determined by the knowledge of σ_k, $(c_k)_{|0}$, E_k, $(c_k)_{|b}$, $c_{i,k\;|+}^*$, and F_k. A different choice for the adjoint solution and/or its boundary conditions would have lead to a different set of sensitivities, as much consistent as the previous one.

4.2. Sensitivities for a typical receptor

Given Eq.(11), the first level sensitivities are essential since they determine the influence of emissions and re-emissions on the measurements at site i. Maps of the mean sensitivities for the years 1997 to 2001, as well as a five years average are drawn on Fig.(5) for Pallas (Finland) and on Fig.(6) for Topolniky (Slovakia). The moderate variability of the sensitivity from year to year is clear. However year 2001 does not seem very representative of all years. As Pallas is off-centre, the sensitivity is influenced by the borders, as opposed to the sensitivity of Topolniky. The yearly averaged adjoint solutions are of diffusive nature as advection processes act as diffusion in the long term. However they are of super-diffusive nature. As a consequence spatial decrease from the site location should be proportional to the inverse of the distance r to some power α. For Fickian diffusion, α is one. Here it is about 2.4, consistent with the exponent that three-dimensional turbulence Kolmogorov power law would yield theoretically. Practically, the yearly-mean influence of a remote source is much weaker on a receptor than predicted by a naive analysis based on Fickian diffusion. This is illustrated in Fig.4.

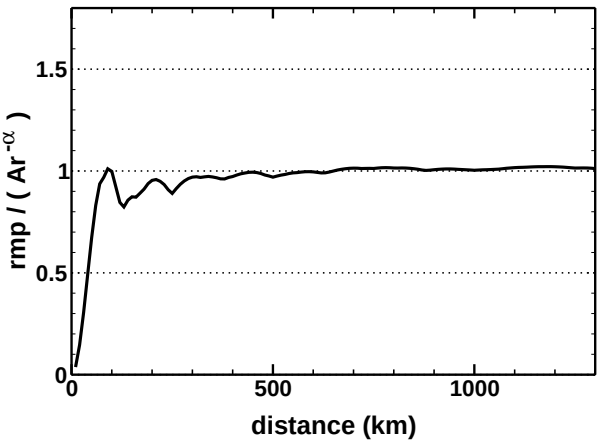

Figure 4. Ratio of the radial mean profile (rmp) of the retroplume from the receptor at Deuselbach (DE04) (averaged over the directions and five years of simulation) to a reference profile $A.r^{-\alpha}$ with $\alpha \simeq 2.4$, with A chosen such that the ratio is 1 at $r = 1000$ km.

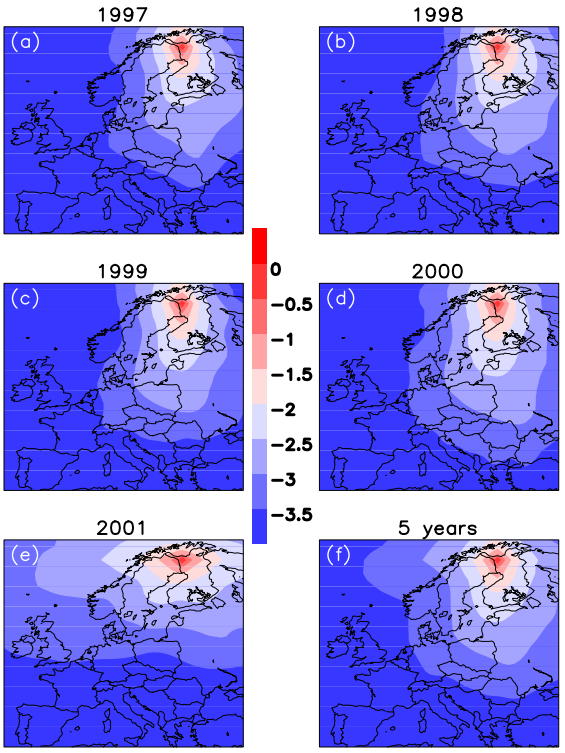

Figure 5. $\log_{10}(\bar{s}/\bar{s}_{\max})$, where $\bar{s}$ is either the annual average emission sensitivity ((a),(b),(c),(d) and (e)) or the five years average emission sensitivity (f) and $\bar{s}_{\max}$ the maximum over the domain of the five years average emission sensitivity, for the receptor site FI96 located at Pallas (Finland).

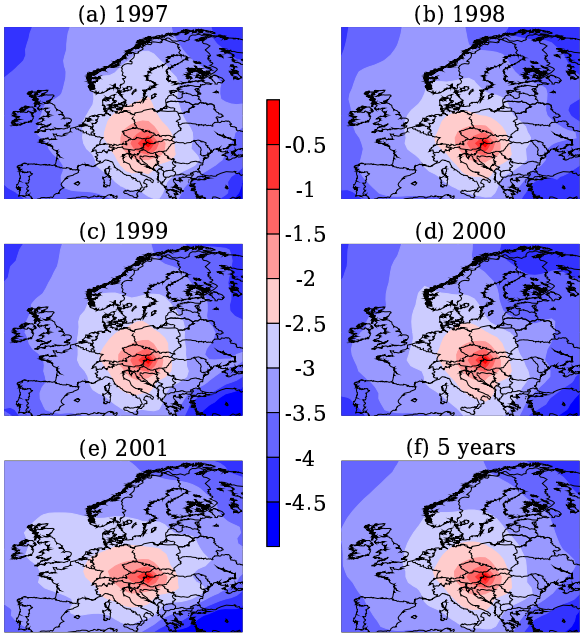

Figure 6. $\log_{10}(\bar{s}/\bar{s}_{\max})$, where $\bar{s}$ is either the annual average emission sensitivity ((a),(b),(c),(d) and (e)) or the five years average emission sensitivity (f) and $\bar{s}_{\max}$ the maximum over the domain of the five years average emission sensitivity, for the receptor site SK07 located at Topolniky (Slovakia).

Slices of the adjoint solution on the borders of the domain, as well as the final bulk state are sensitivities for the incoming advected GEM fluxes and the GEM initial concentrations. Typical examples of such slices are given in Fig.(7). The first graph (a) of this panel represents the average sensitivity to the North face of the domain, for the obervation site FI96. For site SK07, in central Europe, the sensitivity is clearly much weaker (graph (b)) but also much more diffuse. Graphs (c) and (d) represent sensitivities to the initial state for site SK07 for a five years experiment and a one year experiment respectivily. As expected, sensitivities for a five years integration are about five times weaker then for a one-year integration.

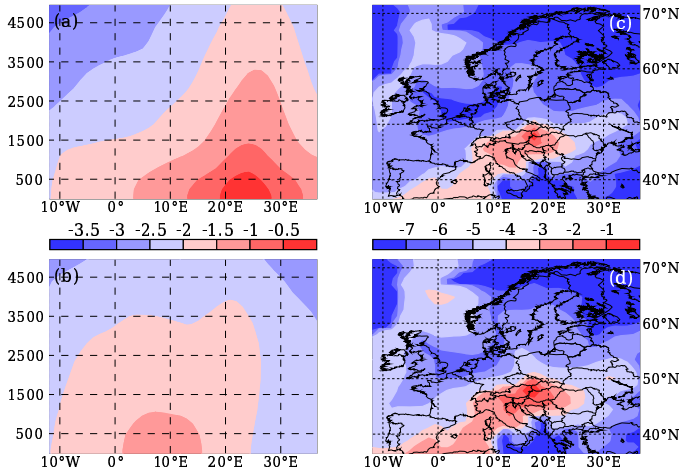

Figure 7. $\log_{10}(\bar{s}/\bar{s}_{\max})$. For (a) and (b), $\bar{s}$ is the five years average sensitivity to the North face of the domain for the receptor site FI96 (a) and SK07 (b). $\bar{s}_{\max}$ is the maximum over the North face (located at 72° N) of $\bar{s}$ for receptor FI96. For (c) and (d), $\bar{s}$ is the initial state sensitivity in SK07 for five years and for one year ((c) and (d) respectively). $\bar{s}_{\max}$ is the maximum over the domain of the initial state sensitivity for one year ((c) and (d)).

4.3. Transboundary transport sensitivity analysis

Transboundary pollution by mercury inside Europe has been studied in (Ilyin et al. [2003]). It was emphasised that the mercury reduction impact was impeded by transboundary transport between countries with a still high level of emission and countries with a significant reduction. The sensitivity analysis advocated here can tell how sensitive a country is to the rest of Europe. To do so, the sampling function π_i is chosen as the support function of the country considered. It also allows for another way to compute the impact of European emissions on the country via the duality relation (Eq.(13) and Eq.(14)).

Some examples of sensitivities are given for Germany, France and the Czech Republic in Fig.8.

The Czech Republic has a low level of mercury emission but is strongly affected by transboundary pollution coming from East Germany and Poland (Ilyin et al. [2003]). Figure 8 helps quantify this potential influence coming from meteorological conditions, geography, and mercury dispersion (actually any influence but the magnitude of the emissions). It clearly demonstrates by numbers the sensitivity of the Czech Republic to its neighbors. Temporal variabilities of

these sensitivities are also illustrated (average over 2001 and the first three months of 2001).

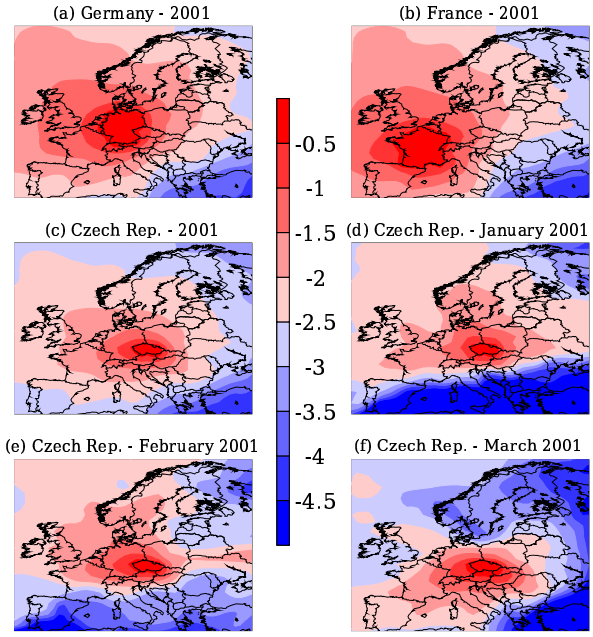

Figure 8. $\log_{10}(\bar{s}/\bar{s}_{\max})$, where $\bar{s}$ are the trans-boundaries annual emission sensitivities for Germany (a), France (b) and the Czech Republic (c). In the case of the Czech Republic examples of monthly averaged sensitivities are also given to demonstrate the intra-year variability of the sensitivity ((d), (e) and (f)). $\bar{s}_{\max}$ is the maximum over the domain of the annual average emission sensitivity for the considered country.

4.4. A specific application to the sensitivity analysis

SE02 is a mercury station located at Rörvik, Sweden and is part of the EMEP heavy metals survey network. The concentration level measured at the very beginning of 2001 is quite difficult to explain by modeling. Predicted mean concentrations for January are about 2.3 ng.m^{-3}, quite far from the 1.5 ng.m^{-3} observed. The contribution of the average simulated concentration in the second half of January (see table 2) gives a source and emission total of 0.75 ng.m^{-3}, an advected contribution of 1.56 ng.m^{-3}, while the contribution from the initial condition is negligible. The emission and source contributions level is high for this latitude. The weak influence of the initial condition, in striking contrast with its contribution for a full January average concentration is consistent with spin-up studies (Roustan and Bocquet [2005]).

Table 2. Concentration contributions (in ng.m^{-3}) at Rörvik at the beginning of 2001 : anthropogenic sources (Sour.), anthropogenic emissions (Ant.), natural emissions (Nat.), re-emissions (Ree.), initial condition (IC), incoming from the top, South, North, West, East, (Top, South, North, West, East), and the total sum (Sum).

	Sour. Top	Ant. South	Nat. North	Ree. West	IC East	Sum
Second half of	0.25	0.26	0.16	0.08	0.002	
January 2001	0.03	0.09	0.09	1.24	0.15	2.35
January	0.19	0.20	0.12	0.06	0.23	
2001	0.02	0.05	0.10	1.18	0.08	2.21

Assume this discrepancy cannot be explained by representativeness flaw or reliability of the measurement. On Fig.9 is represented the profile of mercury concentration near Rörvik in January 2001, as simulated by Polair3D. There is obviously a long episode of mercury pollution in the second half of January.

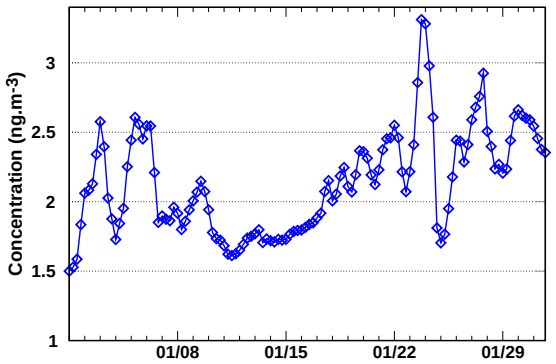

Figure 9. Simulated temporal profile of the gaseous elemental mercury concentration at Rörvik (in ng.m^{-3}).

Then an interesting application of the methods developed so far would be to study the sensitivity of the measurement to emissions. We have computed the sensitivity of the measurement at Rörvik in the last two weeks of January to the emissions. The results, average over time is represented on Fig. (10) and is compared to the analog sensitivity computed for June 2001.

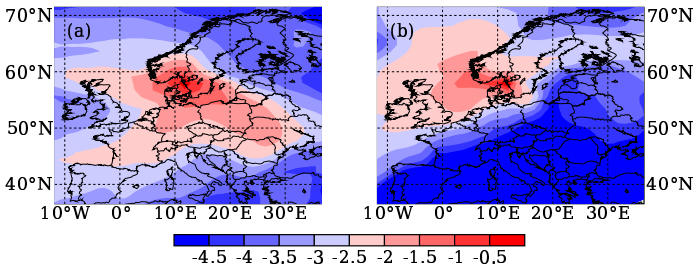

Figure 10. $\log_{10}(\bar{s}/\bar{s}_{\max})$, where $\bar{s}$ is the annual average emission sensitivity of the measurement at Rörvik. This measurement is the average concentration in the second half of January 2001 (a) and June 2001 (b). $\bar{s}_{\max}$ is the maximum over the domain of the annual average emission sensitivity.

For January 2001, in sharp contrast to June 2001, the strong sensitivity to the Germany/Poland area is striking. This area is strongly emitting mercury (see Fig. 11). Since

the sensitivity and the emissions maps are concurrently strong in this region, the very high measurement at Rörvik is not that surprisingly. The representativeness of this particular measurement can therefore be questioned. Part of the discrepancy can nevertheless be explained by a more complex chemistry (Roustan et al. [2005]).

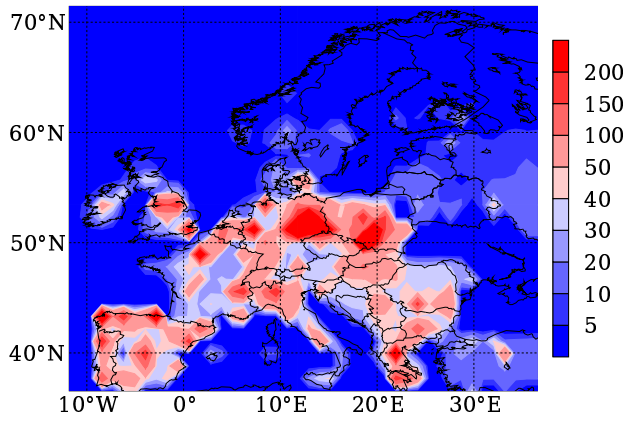

Figure 11. Typical annual emissions in μg.m^{-2}.yr^{-1} tabulated from the EMEP database and used by the simulations.

5. Sensitivity analysis with a more complex mercury chemistry

The mercury model, based on Petersen's scheme, used so far only coped with GEM. To describe the oxidized species dispersion, it is necessary to take into account a more complex chemical scheme.

For instance, in (Roustan et al. [2005]) the analysis lead to seven effective species. Oxidation reactions of Hg(0) within the gaseous phase can produce HgO, HgCl2, and Hg(OH)2. HgO, the agregate species Hg(II), the particulate mercury HgP and Hg(0) interact in the aqueous phase via redox reactions and/or adsorption/desorption processes. From the modeler's perpective, this chemistry is linear in the mercury species, although it involves other species such as SO_2, O_3, OH, etc, which are forced into the model. The chemistry and transport equation now reads :

$$\frac{\partial \boldsymbol{c}}{\partial t} + \mathrm{div}\,(\boldsymbol{u}\boldsymbol{c}) - \mathrm{div}\,(\boldsymbol{K}\nabla\boldsymbol{c}) + \boldsymbol{\Lambda}\,\boldsymbol{c} + \boldsymbol{M}\,\boldsymbol{c} = \sigma\,. \qquad (21)$$

$\boldsymbol{c}$ is the vector of mercury species (seven components in the model mentioned above). $\boldsymbol{\Lambda}$ is the diagonal matrix of the scavenging coefficient (species-dependent). $\boldsymbol{M}$ is the kinetic matrix describing the first-order (in mercury) chemistry and depends on forced fields of other species concentration.

To generalize the adjoint analysis performed with the GEM model, it is convenient to introduce the canonical scalar product in the space of mercury species : $\langle \boldsymbol{x}, \boldsymbol{y}\rangle = \boldsymbol{x}^T\boldsymbol{y}$. The measurement equation is now :

$$\mu_i = \int_\Omega \mathrm{d}t\mathrm{d}\boldsymbol{x}\,\langle \boldsymbol{\pi}_i(\boldsymbol{x},t), \boldsymbol{c}(\boldsymbol{x},t)\rangle\,. \qquad (22)$$

The sampling function $\boldsymbol{\pi}_i$ is a vector in the space of species. The retro-transport equation generalizes to :

$$-\frac{\partial \boldsymbol{c}_i^*}{\partial t} - \mathrm{div}\,(\boldsymbol{u}\boldsymbol{c}_i^*) - \mathrm{div}\,(\boldsymbol{K}\nabla\boldsymbol{c}_i^*) + \boldsymbol{\Lambda}\boldsymbol{c}_i^* + \boldsymbol{M}^T\boldsymbol{c}_i^* = \boldsymbol{\pi}_i\,. \qquad (23)$$

For a concentration measurement such as the one described by Eq.(22), the adjoint analysis is similar and one obtains

$$\mu_i = \int_\Omega \mathrm{d}t\mathrm{d}\boldsymbol{x}\,\langle \boldsymbol{c}_i^*, \boldsymbol{\sigma}\rangle + \int_{\partial\Omega_0} \mathrm{d}\boldsymbol{x}\,\langle \boldsymbol{c}_i^*, \boldsymbol{c}\rangle + \int_{\partial\Omega_b} \mathrm{d}t\mathrm{d}\boldsymbol{S}\cdot(\langle \boldsymbol{c}, \boldsymbol{J}_i^*\rangle - \langle \boldsymbol{c}_i^*, \boldsymbol{J}\rangle) - \int_{\partial\Omega_+} \mathrm{d}t\mathrm{d}\boldsymbol{S}\cdot(\langle \boldsymbol{c}_i^*, \boldsymbol{c}\rangle\boldsymbol{u})\,. \qquad (24)$$

Since the complex model incorporates explicitly oxidized species, the dry and wet deposition flux of mercury can now be estimated properly, and are more relevant observable quantities. How does the adjoint analysis generalize to these types of measurements is the object of the following development.

5.1. Sensitivity of wet scavenging

The wet flux measurement equation is

$$\nu_i^{\mathrm{w}} = \int_\Omega \mathrm{d}t\mathrm{d}\boldsymbol{x}\,\langle \boldsymbol{\pi}_i(\boldsymbol{x},t), \boldsymbol{c}(\boldsymbol{x},t)\rangle\,, \qquad (25)$$

where ν_i^{w} is a mass flux measurement (in kg.m^{-2}.s^{-1}). Here $\boldsymbol{\pi}_i$ is the vector of scavenging rates $\lambda(\boldsymbol{x},t)$ in m^{-2}.s^{-2} : a rate of loss, per unit of time of the physical process, per unit of time of the measurement, and per unit of surface where the mercury is accumulated. Those rates are directly related to the scavenging coefficients of $\boldsymbol{\Lambda}$. Then the adjoint analysis stands with this new $\boldsymbol{\pi}_i$, and ν_i can be expressed in the way μ_i was. Contrary to a ground concentration measurement the simulation of the adjoint solution of a wet deposition measurement implies having sources in the cells of the column above the deposition plaquette (base of the ground cell) but in and below cloud. $\boldsymbol{\pi}_i$ is of the typical form

$$\boldsymbol{\pi}_i(\boldsymbol{x}) = (\lambda_1, \cdots, \lambda_s)^T\,\delta(x - x_i)\,\delta(y - y_i) \qquad (26)$$

for an annual mean measurement (s is the number of species).

The sensitivity of the wet deposition flux of all mercury species to one of them is given by the components in the space of species of the vector field $\boldsymbol{c}_i^*$. This set of sensitivities can be obtained numerically with one single run.

5.2. Sensitivity of dry deposition

The construct is a bit more elaborate in the case of dry deposition since it is usually included in the boundary conditions of a numerical model. The dry flux observation equation is

$$\nu_i^{\mathrm{d}} = \int_{\partial\Omega_b} \mathrm{d}t\mathrm{d}S\,\langle \boldsymbol{V}_i^{\mathrm{dep}}(\boldsymbol{x},t), \boldsymbol{c}(\boldsymbol{x},t)\rangle\,, \qquad (27)$$

where ν_i^{d} is a mass flux measurement. $\boldsymbol{V}_i^{\mathrm{dep}}$ is the vector of the velocity deposition per unit of surface where it is deposited and unit of time measurement (in units of m^{-1}.s^{-2}). It is directly related to the usual deposition velocity v^{dep} in units of m.s^{-1}. We now choose :

$$\boldsymbol{n}\cdot\boldsymbol{J}_i^* = v^{\mathrm{dep}}\boldsymbol{c}_{i|b}^* - \boldsymbol{V}_i^{\mathrm{dep}}\,. \qquad (28)$$

Until now the sampling function $\boldsymbol{\pi}_i$, was used as the volume emission term of the retro-transport equation. Since the observation term for dry flux can be expressed through a different choice for $\boldsymbol{J}_i^*$ its becomes natural to take it null. As a consequence, one obtains

$$\nu_i^{\mathrm{d}} = \int_\Omega \mathrm{d}t\mathrm{d}\boldsymbol{x}\,\langle \boldsymbol{c}_i^*, \boldsymbol{\sigma}\rangle + \int_{\partial\Omega_0} \mathrm{d}\boldsymbol{x}\,\langle \boldsymbol{c}_i^*, \boldsymbol{c}\rangle + \int_{\partial\Omega_b} \mathrm{d}t\mathrm{d}\boldsymbol{S}\cdot\langle \boldsymbol{c}_i^*, \boldsymbol{E}\rangle - \int_{\partial\Omega_+} \mathrm{d}t\mathrm{d}\boldsymbol{S}\cdot(\langle \boldsymbol{c}_i^*, \boldsymbol{c}\rangle\boldsymbol{u})\,. \qquad (29)$$

By the superposition principle it easy to generalize to the case where both wet and dry deposition are measured simultaneously at a given site.

As a conclusion, the sensitivities of a dry deposition flux are therefore modeled via a virtual ground emission $\boldsymbol{V}_i^{\text{dep}}$ in the calculation of the adjoint solution.

5.3. Application

Here is presented the analysis of the sensitivity of mercury measurements to several mercury species emissions at the EMEP site Rörvik. The first set of maps Fig.12 represents the sensitivity of an Hg(0) annual average concentration in the air at Rörvik.

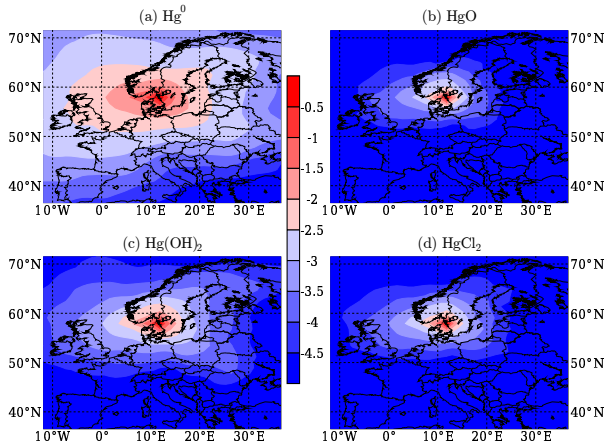

Figure 12. $\log_{10}(\bar{s}/\bar{s}_{\max})$, where $\bar{s}$ are annual average sensitivities of the gaseous mercury concentration at Rörvik, to Hg(0) (a), HgO (b), $Hg(OH)_2$ (c), and $HgCl_2$ (d) emissions. $\bar{s}_{\max}$ is the maximum over the domain of the annual average sensitivity to Hg(0) emissions.

The patterns obtained emphasized the disparities in atmospheric residence time of the mercury species. Sensitivity gradient are clearly stronger for the oxidized species, the short-lived ones. Although the potential contribution of these species emissions to GEM concentration measurement appears locally not negligible, emissions of Hg(0) remains the most influential.

The second panel Fig.13 represents the sensitivity of annual flux of total deposited mercury by wet scavenging at Rörvik.

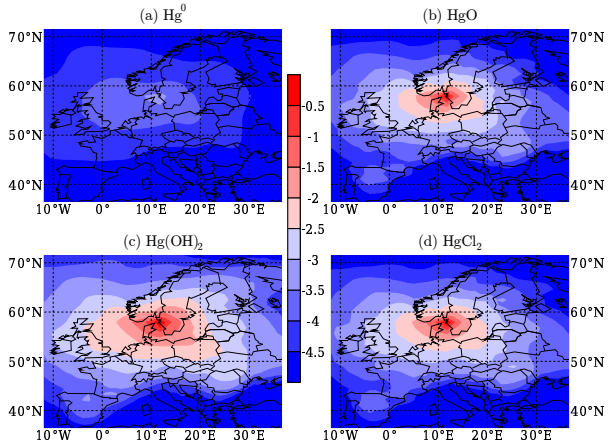

Figure 13. $\log_{10}(\bar{s}/\bar{s}_{\max})$. $\bar{s}$ are annual average sensitivities of the wet deposition flux at Rörvik, to Hg(0) (a), HgO (b), $Hg(OH)_2$ (c), and $HgCl_2$ (d) emissions. $\bar{s}_{\max}$ is the maximum over the domain of the annual average sensitivity to $HgOH_2$ emissions.

Here the situation is the opposite to the previous one. The weak solubility of gaseous elemental mercury leads to a poor sensitivity of the wet deposition flux measurement to Hg(0) surface emissions. This result agrees with the consensus (Ryaboshapko et al. [1998]) ascribing the main part of the mercury deposited mass by rain to the wet scavenging of oxidized species. The area of relatively strong sensitivity over Spain may be explained by its semi-arid climate. High surface temperature and rare precipitation, especially during summer, promote transport at higher heights than for temperate conditions. In the process, a lesser mass of oxidized mercury is removed by dry deposition and is then likely to be washed out by rain later on.

The third panel Fig.14 represents the sensitivity of annual flux of total deposited mercury by dry deposition at Rörvik.

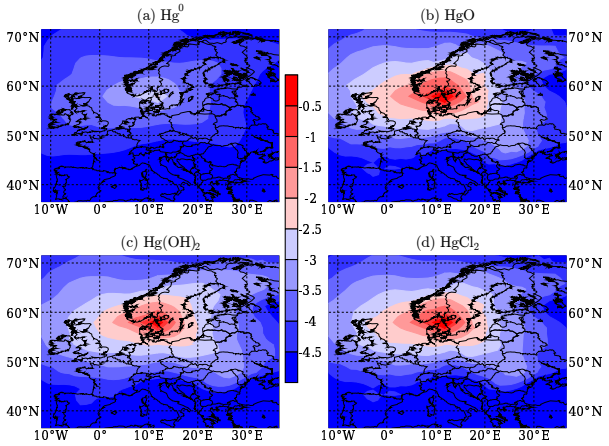

Figure 14. $\log_{10}(\bar{s}/\bar{s}_{\max})$. $\bar{s}$ are annual average sensitivities of the dry deposition flux at Rörvik, to Hg(0) (a), HgO (b), $Hg(OH)_2$ (c), and $HgCl_2$ (d) emissions. $\bar{s}_{\max}$ is the maximum over the domain of the annual average sensitivity of the wet deposition (Fig.13) to $HgOH_2$ emissions.

Here again the deposition flux measurement is more sensitive to surface emissions of oxidized species. This is not surprising since high solubility and adsorption facilitate dry deposition processes.

It is clear that the sensitivity of dry deposition is higher close to the measurement site, compared to wet deposition (contour plots of Fig.13 and Fig.14 are normalized by the same value). However a few hundred kilometers away from the station and beyond, the sensitivity of wet deposition flux turns prominent.

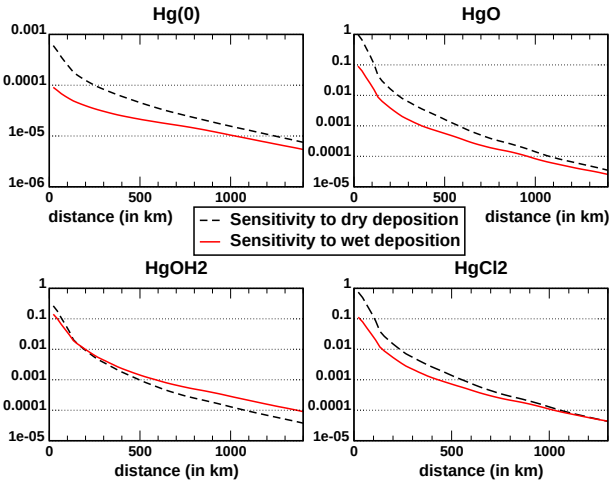

Figure 15. Radial mean profile of the sensitivities of dry and wet deposition to emissions at Rörvik, to Hg(0), HgO, $Hg(OH)_2$, and $HgCl_2$. The sensitivities are normalized by the maximum of all the sensitivities (dry - $Hg(OH)_2$). The distance to the measurement site is given in km.

This last result shows that the prominent deposition process at a given place and for a given chemical is not only determined by the local meteorological conditions but also by the distance from the emission area to this place. Whether the dry or wet deposition process is prominent depends on the oxidized form (see Fig.15).

The gaseous oxidized species, HgO, $Hg(OH)_2$, and $HgCl_2$ have distinct solubility, which is their main discriminating factor with respect to the removal processes. In the model, solubilities are described via the Henry's law constant of the species, respectively (in $mol.L^{-1}.atm^{-1}$) 2.7×10^{12} (Schroeder and Munthe [1998]), 1.2×10^4 and 1.4×10^6 (Lindqvist and Rodhe [1985]).

The scavenging coefficients computed for HgO, $Hg(OH)_2$, and $HgCl_2$ are obviously correlated in space and time, moreover they are of the same order of magnitude. Consequently wet scavenging has very similar impact on the different gaseous oxidized species during their atmospheric transport.

On the other hand dry deposition velocities are much more sensitive to the Henry constant values. The sensitivity of dry deposition is roughly the product of the local dry deposition magnitude with the transport and removal processes along the way from the emission area to the receptor. A higher value of the Henry constant (stronger solubility) increases the first factor independently of the transport, and moves up the dry deposition sensitivity radial profile. Moreover a higher solubility comes into the second factor as it implies a stiffer slope of the profile, since the species is even more deposited along its way to the receptor. For the same reason, the wet deposition sensitivity profile stiffness depends on the solubility, but through the dry deposition process (the mass removed by dry deposition process is not any more available to be washed out by precipitation).

In summary, the results presented in Fig.12 suggest an appreciable role of the boundary conditions for Hg(0) air concentrations estimate as in the case of the simple chemistry model. However determination of deposition fluxes seems to be much more sensitive to the local emissions speciation (Fig.13 and Fig.14), which is in agreement with results presented in (Pai et al. [1999]). A sensitivity analysis based on the indirect approach is presented in (Travnikov and Ilyin [2005]) for a mercury model over Europe. It emphasizes the crucial role played by GEM boundary conditions in evaluating mercury air concentrations, but also for deposition fluxes. It would be interesting to proceed to a comparison between results from indirect and from adjoint method. However such a comparison is not immediate and goes beyond the scope of this work.

6. Conclusions

In this paper, we have developed tools for the sensitivity analysis of mercury transport and fate within a regional model domain. To do so we have introduced adjoint solutions of the transport taking into account the initial and boundary conditions. The adjoint solution decomposes into as many parts as the number of forcings (initial conditions, boundary conditions, emissions). The method developed here differs significantly from the previously used techniques, such as the indirect approach in mercury studies, or the DDM method in other air quality models. It allows to computes in a single run comprehensive and quantitative maps of sensitivities for a given observation. This is less straightforward with the methods mentioned earlier.

Those computations were first performed for gaseous elemental mercury using the Petersen scheme as a simplified mercury chemistry. At first, the method was applied to the analysis of the sensitivity of a specific receptor, using the numerical model POLAIR3D. For annual mean measurements, the sensitivity was shown to decrease like a power law with the distance r to a source like $r^{-2.4}$, much faster than would a Fickian dispersion. The technique was then applied to the transboundary dispersion problem. In particular the method allows to compute very efficiently the sensitivity of averaged mercury concentrations over a country to exterior sources, and, in the case of a regional model, incoming fluxes of mercury. Computations are performed

for the Czech Republic, France and Germany for the year 2001.

In order to account for the oxidized species dispersion and deposition, the method was then generalized to a more complex chemistry. Although it is implemented with POLAIR3D in this work, the method is general and valid for any Eulerian model of mercury transport. In particular, using such a chemistry, it was shown how to calculate sensitivities of the dry and wet deposition fluxes to any of the forcings. Relative sensitivities of the two removal processes were examined.

In perspective for future works, we would like to point out to two main leads.

Firstly, the computation of the adjoint solutions allows for a direct representation of the measurements in terms of the forcings. Therefore it could be used to attempt inverse modeling of some of the forcings (essentially boundary conditions and emissions).

Secondly, in the paper, relying on the linearity of the model, we have computed sensitivities to parameters which are linearly connected to the measurements. However, the method could be partially extended to cope with parameters such as a kinetic rate participating in the mercury chemistry, or a concentration level of oxidizing species (OH, O_3). These are not linearly connected to the measurements.

To see how this could be possible, consider a perturbation in a kinetic rate, or in oxidizing species concentrations, which are encoded in $\boldsymbol{M}$. Then the variational equation which describes the propagation of the perturbation is

$$\frac{\partial \delta \boldsymbol{c}}{\partial t} + \operatorname{div}(\boldsymbol{u}\delta\boldsymbol{c}) - \operatorname{div}(\boldsymbol{K}\nabla\delta\boldsymbol{c}) + \boldsymbol{\Lambda}\delta\boldsymbol{c} + \boldsymbol{M}\delta\boldsymbol{c} = -(\delta\boldsymbol{M})\boldsymbol{c}\,, \tag{30}$$

where δ denotes first-order variations, and $\boldsymbol{c}$ and $\boldsymbol{M}$ are leading order quantities. Initial and boundary conditions are null for $\delta\boldsymbol{c}$. Then it can be shown that the variation of the measurement at site (i) is

$$\begin{aligned} \delta\mu_i &= \int_\Omega \mathrm{d}t\mathrm{d}\boldsymbol{x}\, \langle \boldsymbol{\pi}_i(\boldsymbol{x},t), \delta\boldsymbol{c}(\boldsymbol{x},t)\rangle \\ &= \int_\Omega \mathrm{d}t\mathrm{d}\boldsymbol{x}\, \langle \boldsymbol{c}_i^*, (\delta\boldsymbol{M})\boldsymbol{c}\rangle, \end{aligned} \tag{31}$$

From this formula can be simply read out the first-order sensitivities to one of the parameters entering $\boldsymbol{M}$. It depends on the concentrations vector field $\boldsymbol{c}$ as the perturbation depends non-linearly on the two types of parameters mentioned previously. It also depends on the adjoint solutions, that may have been previously computed for other sensitivity analysis (using the leading order kinetic matrix $\boldsymbol{M}$). Note that in this particular case, there is no boundary contributions. Therefore this method could also be used to calculate (at least) first-order sensitivity to parameters non-linearly related to concentrations.

The authors wish to thank B. Sportisse, and L. Musson-Genon for encouragement and discussions. Y. Roustan acknowledges financial support from ADEME and EDF.

Appendix A: Statistical indicators

Here are defined the statistical indicators used in this work. Consider a set of concentration measurements $\mu_{i=1,\cdots,p}$, and a set of predicted values for those measurements $c_{i=1,\cdots,p}$. Define the means

$$\overline{\mu} = \frac{1}{p}\sum_{i=1}^{p}\mu_i \qquad \text{and} \qquad \overline{c} = \frac{1}{p}\sum_{i=1}^{p} c_i\,, \tag{A1}$$

and the bias and the fractional bias (FB) are defined by

$$\overline{\mu} - \overline{c} \quad \text{and} \quad 2\,\frac{\overline{\mu}-\overline{c}}{\overline{\mu}+\overline{c}}\,. \tag{A2}$$

The normalized root mean square is

$$\sqrt{\frac{1}{p}\sum_{i=1}^{p}\frac{(\mu_i - c_i)^2}{\overline{\mu}\,\overline{c}}}\,, \tag{A3}$$

and eventually the individually normalized root mean square is

$$\sqrt{\frac{1}{p}\sum_{i=1}^{p}\frac{(\mu_i - c_i)^2}{\mu_i c_i}}\,. \tag{A4}$$

References

Aas, W. and Hjellbrekke, A.G.: Heavy metals and POP measurements, 2001. EMEP/CCC report 1/2003, 2003.

Ariya, P.A., Dastoor, A.P., Amyot, M., Schroeder, W.H., Barrie, L., Anlauf, K., Raofie, F., Ryzhkov, A., Davignon, D., Lalonde, J. and Steffen, A.: The Arctic: a sink for mercury. *Tellus*, *56B*, 397–403, 2004.

Baer, M. and Nester, K.: Parameterization of trace gas dry deposition velocities for a regional mesoscale diffusion model. *Annales Geophysicae*, *10*, 912–923, 1992.

Boutahar, J., Lacour, S., Mallet, V., Quélo, D., Roustan, Y. and Sportisse, B.: Development and validation of a fully modular platform for numerical modelling of air pollution: POLAIR. *Int. J. Environment and Pollution*, *22(1/2)*, 17–28, 2004.

Brook, J.R., Zhang, L., Di-Giovanni, F. and Padro, J.: Description and evaluation of a model of deposition velocities for routine estimates of air pollutant dry deposition over North America. Part I: model development. *Atmos. Environ.*, *33*, 5037–5051, 1999.

Bullock, O.R. and Brehme, K.A.: Atmospheric mercury simulation using the CMAQ model: formulation description and analysis of wet deposition results. *Atmos. Environ.*, *36*, 2135–2146, 2002.

Carmichael, G.R., Sandu, A., and Potras, F.A.: Sensitivity analysis for atmopheric chemistry models via automatic differentiation. *Atmos. Environ.*, *31*, 475–489, 1997.

Christensen, J.H., Brandt, J., Frohn, L.M. and Skov,H.: Modelling of mercury with the Danish Eulerian Hemispheric Model. *Atmos. Chem. Phys.*, *4*, 2251–2257, 2004.

Cosme, E., Hourdin, F., Genthon, C., Martinerie, P.: The origin of dimethylsulfide, non-sea-salt sulfate, and methanesulfonic acid in Eastern Antartica. *J. Geophys. Res.*, *110*, D03302, 2005.

Daescu, D.N. and Carmichael, G.R.: An adjoint sensitivity method for the adaptive location of the observations in air quality modeling. *J. Atmos. Sci.*, *60(2)*, 434–450, 2003.

Dunker, A., Yarwood, G., Ortman, J.P., and Wilson, G.M.: The decoupled direct method for sensitivity analysis in a three-dimensional air quality model - Implementation, accuracy, and efficiency. *Environ. Sci. Technol.*, *36*, 2665–2976.

Elbern, H., and Schmidt, H.: A four-dimensional variational chemistry data assimilation scheme for eulerian chemistry transport modeling. *J. Geophys. Res.*, *104*, 18583–18598, 1999.

Hall, B.: The gas phase oxidation of elemental mercury by ozone. *Water, Air Soil Pollut.*, *80*, 301–315, 1995.

Hicks, B.B. and Liss, P.S.: Transfer of SO_2 and other reactive gases across the air-sea interface. *Tellus*, *28*, 348–354, 1976.

Hourdin, F., Talagrand, O. and Idelkadi, A.: Eulerian bactracking of Atmospheric tracers: II Numerical aspects. Sumitted to *Q.J.R. Meteorol. Soc.*, 2005.

Ilyin, I., Ryaboshapko A. and Travnikov, O.: Heavy metal contamination on European and Hemisperical scale. EMEP Status report 3/2002, 2002.

Ilyin, I., Travnikov, O., Aas, W. and Uggerud,H.Th.: Heavy metals: transboundary pollution of the environment. EMEP Status report 2/2003, 2003.

Kaminski, T., Heinmann, M., and Giering, R.: A coarse grid three-dimensional global inverse model of the atmospheric transport: I adjoint model and jacobian matrix. *J. Geophys. Res.*, *104*, 18535–18553, 1999.

Lin, X. and Tao, Y.: A numerical modelling study on regional mercury budget for eastern North America. *Atmos. Chem. Phys. Discuss.*, *3*, 983–1015, 2003.

Lindqvist, O. and Rodhe, H.: Atmospheric mercury - a review. *Tellus*, *37B*, 136–159, 1985.

Liu, W., Hopke, P.K, Han, Y., Yi, S.M., Holsen, T.M., Cybart, S., Kozlowski, K. and Milligan, M.: Application of receptor modeling to atmospheric constituents at Potsdam and Stockton, NY. *Environ. Sci. Technol.*, *38*, 555–569, 2004.

Mallet, V. and Sportisse, B.: 3-D chemistry-transport model Polair: numerical issues, validation and automatic-differentiation strategy. *Atmos. Chem. Phys. Discuss.*, *4*, 1371–1392, 2004.

Marchuk, G. I.: Adjoint equations and Analysis of Complex Systems. Mathematics and its Applications, Hazewinkel (Ed), Kluwer Academic Publisher, 1995.

Pai, P., Karamchandani, P., Seigneur, C.: Sensitivity of simulated atmospheric mercury concentrations and depositions to model input parameters. *J. Geophys. Res.*, *104*, 13855–13868, 1999.

Petersen, G, Iverfeldt, A. and Munthe, J.: Atmospheric mercury species over central and northern Europe. Model calculations and comparison with observations from the nordic air and precipitation network for 1987 and 1988. *Atmos. Environ.*, *29*, 47–67, 1995.

Roselle, S.,J. and Binkowski, F.,S.: Science Algorithms of the EPA Models-3 Community Multiscale Air Quality (CMAQ) Modeling System, EPA/600/R-99/030, Chap. 11, March 1999.

Roustan, Y., Bocquet, M., Musson Genon, L., Sportisse, B.: Modeling atmospheric mercury at European scale with the Chemistry Transport Model Polair3D. *Proceedings of Gloream 2004*, 2005.

Roustan, Y. and Bocquet, M.: Inverse modeling of mercury over Europe, submitted to Atmos. Chem. and Phys., 2005.

Ryaboshapko, A., Ilyin, I., Gusev, A. and Afinogenova, O.: Mercury in the atmosphere of Europe: concentrations, deposition patterns, transboundary fluxes. EMEP/MSC-E Report 7/1998, 1998.

Ryaboshapko, A., Bullock, R., Ebinghaus, R., Ilyin, I., Lohman, K., Munthe, J., Petersen, G., Seigneur, C. and Wngberg, I.: Comparison of mercury chemistry models. *Atmos. Environ.*, *36*, 3881–3898, 2002.

Sartelet, K., Boutahar, J., Quélo, D., Coll, I., Plion, P. and Sportisse, B: Development and Validation of a 3D Chemistry-Transport Model, POLAIR3D, by Comparison with Data from ESQUIF Campaign. Proceedings of the 6th Gloream workshop: Global and regional atmospheric modeling, 140–146, 2002.

Schroeder, W.H. and Munthe, J.: Atmospheric mercury - an overview. *Atmos. Environ.*, *32*, 809–822, 1998.

Seigneur, C., Karamchandani, P., Lohman, K., Vijayaraghavan, K. and Shia, R.L.: Multiscale modeling of the atmospheric fate and transport of mercury. *Journal of Geophysical Research*, *106*, 27795–27809, 2001.

Seigneur, C., Karamchandani, P., Vijayaraghavan, K., Lohman, K., Shia, R. and Levin, L.: On the effect of spatial resolution on atmospheric mercury modeling. *The Science of the Total Environment*, *304*, 73–81, 2003.

Seigneur, C., Vijayaraghavan, K., Lohman, K., Karamchandani, P. and Scott, C.: Global source attribution for mercury deposition in the United States. *Environ. Sci. Technol.*, *38*, 555–569, 2004.

Sommar, J., Gårdfeldt, K., Strmberg, D. and Feng, X.: A kinetic study of the gas-phase reaction between the hydroxyl radical and atomic mercury. *Atmos. Envir.*, *35*, 3049–3054, 2001.

Spee, E.: Numerical methods in global transport models. PhD Thesis, Univ. Amsterdam, 1998.

Sportisse, B., Boutahar, J., Debry, E., Quélo, D. and Sartelet, K.: Some tracks in Air Pollution Modeling. POLAIR: a numerical platform for air pollution modeling. *RACSAM Journal of the Spanish Science Academy, Real Academia de Ciencias de Espana*, *96* 507–528, 2002.

Sprotissse, B. and du Bois, L.: Numerical and theoretical investigation of a simplified model for the parameterization of below-cloud scavenging by falling raindrops. *Atmos. Environ.*, *36*, 5719–5727, 2002.

Travnikov, O. and Ilyin, I: Regional model MSCE-HM of heavy metal transboundary air pollution in Europe. EMEP/MSC-E Technical Report 6/2005, 2005.

Uliasz, M.: Application of the perturbation theory to the sensitivity analysis of an air pollution model. *Zeitshrift für Meteorologie*, *33*, 169–181, 1983.

Vuillemier, L., Harley, R.A., and Brown, N.J.: First- and Second-Order Sensitivty Analysis of a Photochemically Reactive System (A Green's Function Approach). *Environ. Sci. Technol.*, *31*, 1206–1217, 1997.

Wesely, M.L. and Hicks, B.B.: A review of the current status of knowledge on dry deposition. *Atmos. Environ.*, *34*, 2261–2281, 2000.

Xu, X., Yang, X., Miller, D.R., Helble, J.J., Thomas, H., Carley, R.J.: A sensitivity analysis on the atmospheric transformation and deposition of mercury in north-eastern USA. *Sci. Total Environ.*, *259*, 169–181, 2000.